

Stacked Josephson junction SQUID

V.M.Krasnov*

Department of Microelectronics and Nanoscience, Chalmers University of Technology, S-41296
Göteborg, Sweden

Operation of a Superconducting Quantum Interference Device (SQUID) made of stacked Josephson junctions is analyzed numerically for a variety of junction parameters. Due to a magnetic coupling of junctions in the stack, such a SQUID has certain advantages as compared to an uncoupled multi-junction SQUID. Namely, metastability of current-flux modulation can be reduced and a voltage-flux modulation can be improved if junctions in the stack are phase-locked. Optimum operation of the SQUID is expected for moderately long, strongly coupled stacked Josephson junctions. A possibility of making a stacked Josephson junction SQUID based on intrinsic Josephson junctions in high- T_c superconductor is discussed.

Keywords: SQUID, stacked Josephson junctions, High- T_c superconductors

PACS: 85.25.Dq, 74.80.Dm, 74.72.Hs

1. Introduction

Layered high- T_c superconductors (HTSC) represent natural stacks of atomic scale intrinsic Josephson junctions (IJJ's) [1]. Indeed, an interlayer spacing of 15.5 \AA was estimated from a periodic Fraunhofer modulation of Fiske steps in Bi-2212 mesas [2]. At present, high quality SIS-type IJJ's can be fabricated using HTSC mesa structures [3,4]. IJJ's with their record large $I_c R_n$ values $\sim 10 mV$ are attractive candidates for cryoelectronics.

Here I analyze a possibility of making a SQUID, based on IJJ's. Because the interlayer spacing in HTSC is very small, it is likely that such a SQUID will contain several stacked Josephson junctions (SJJ's), as shown schematically in Fig. 1. From previous studies it is known that operation of a multi-junction SQUID, consisting of series connected uncoupled junctions, is problematic due to the existence of metastable states and a small current-flux modulation [5–7]. The main difference between series connected and stacked junctions is that SJJ's are coupled with each other, which may result in qualitatively different behavior of SJJ's, see eg. recent review [8].

The main question which is raised in this paper, is whether the operation of a multi-junction

SQUID can be improved by coupling and phase-locking in stacked Josephson junctions.

2. Magnetic coupling in stacked junctions

I will consider a magnetically (inductively) coupled stack of N junctions. The coupling is achieved via common electrodes and is strong when they are thinner than the London penetration depth, λ_S (which is certainly the case for HTSC IJJ's). Properties of magnetically coupled SJJ's are described by a coupled sine-Gordon equation [9],

$$\varphi_i'' = \mathbf{A} \cdot J_i \sin(\varphi_i) - \mathbf{J}_b. \quad (1)$$

Here φ_i are gauge invariant phase differences, 'primes' denote in-plane spatial derivatives, \mathbf{A} is a symmetric tridiagonal $N \times N$ matrix with nonzero elements: $A_{i,i-1} = -S_i/\Lambda_l$; $A_{i,i} = \Lambda_i/\Lambda_l$; $A_{i,i+1} = -S_{i+1}/\Lambda_l$, where $\Lambda_i = t_i + \lambda_{S_i} \coth\left(\frac{d_i}{\lambda_{S_i}}\right) + \lambda_{S_{i+1}} \coth\left(\frac{d_{i+1}}{\lambda_{S_{i+1}}}\right)$, $S_i = \lambda_{S_i} \operatorname{cosech}\left(\frac{d_i}{\lambda_{S_i}}\right)$, d_i and t_i are thicknesses of superconducting electrodes and insulating barriers, respectively, and \mathbf{J}_b is a bias term [10].

The coupling strength S is determined by off-diagonal elements of \mathbf{A} . For identical junctions,

$$S \simeq 2ch^{-1}(d/\lambda_S). \quad (2)$$

*E-mail address: krasnov@fy.chalmers.se

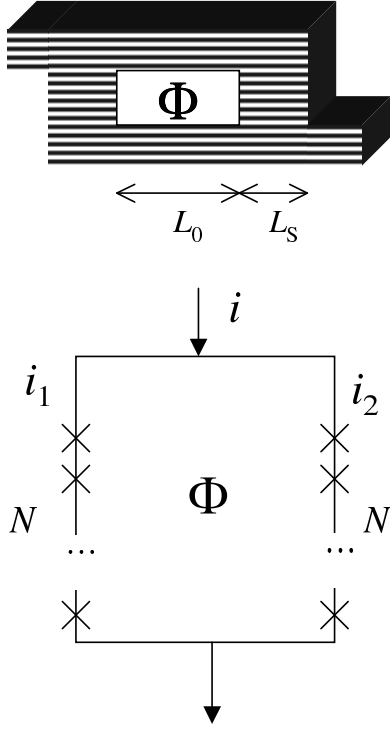


Figure 1. A schematic view and a diagram of a stacked Josephson junction SQUID.

3. Short junctions, $L_S < \lambda_J$

According to Eq.(1), SJJ's are coupled via the second derivative of phase. The characteristic length for the phase variation is given by the Josephson penetration depth, $\lambda_J = \sqrt{\frac{\Phi_0 c}{8\pi^2 J_c \Lambda_S}}$ [8]. For short SJJ's, $L_S < \lambda_J$, magnetic coupling is inefficient and a SJJ SQUID is described by similar expressions as an uncoupled multi-junction SQUID, see the diagram in Fig. 1.

$$i = i_1 + i_2; \quad (3)$$

$$J_{1i} \sin(\varphi_{1i}) = i_1, \quad J_{2j} \sin(\varphi_{2j}) = i - i_1; \quad (4)$$

$$\varphi_{1i} = \arcsin\left(\frac{J_{1k} \sin(\varphi_{1k})}{J_{1i}}\right) + 2\pi n,$$

$$\varphi_{2j} = \arcsin\left(\frac{i - J_{1k} \sin(\varphi_{1k})}{J_{2j}}\right) + 2\pi m; \quad (5)$$

$$\Phi = \frac{\Phi_0}{2\pi} \left[\sum \varphi_{1i} - \sum \varphi_{2j} \right]. \quad (6)$$

Here subscripts 1 and 2 correspond to left and right legs of the SQUID, respectively, $\Phi = \Phi_e - i_1 L_1 + i_2 L_2$ is the total magnetic flux in the SQUID loop, Φ_e is an external flux and $L_{1,2}$ are inductances of the SQUID legs. All variables are expressed in terms of the phase difference in the weakest junction "1k".

The critical current vs. flux characteristic of the SQUID with $N = 3$ uncoupled ($L_S = 0$) junctions per leg with equal J_c 's is shown in Fig. 2 by thin lines. It is seen that $I_c(\Phi)$ consists of a number of lobes. Each lobe has a width $N\Phi_0$ (not Φ_0 as in a conventional SQUID). This can be easily understood from Eq.(6): due to a summation in the right-hand side, the overall flux increases N -fold as compared to a conventional SQUID with a single junction per leg. Nevertheless, the overall periodicity of the $I_c(\Phi)$ pattern is one flux quantum Φ_0 . This is caused by the appearance of equivalent lobes shifted by Φ_0 , corresponding to 2π shift of phase in the junctions, see Eq.(6).

From such a simple analysis we can see two main disadvantages of the uncoupled multi-junction SQUID: (i) The SQUID possesses several metastable states and $I_c(\Phi)$ is not unique, (ii) The overall modulation of $I_c(\Phi)$ (envelope of all lobes) strongly decreases due to a mismatch between the width of the individual lobe ($N\Phi_0$) and the spacing between lobes (Φ_0).

4. Long junctions, $L_S > \lambda_J$

Magnetic coupling is effective in long stacks. However, as far as SQUID application is concerned, the stack should not be too long otherwise flux penetration inside the stack becomes complicated due to the appearance of multiple quasi-equilibrium fluxon modes [10,11,8]. The optimum stack should have a moderate length, $L_S \sim 4\lambda_J$, so that magnetic coupling is effective, but fluxon modes in SJJ's are not pronounced.

Static current-flux characteristics of a SJJ SQUID with the geometry shown in Fig.1 were simulated numerically using a finite difference method with successive interactions. For each stack, Eq. (1) was solved together with Eqs.(3,6)

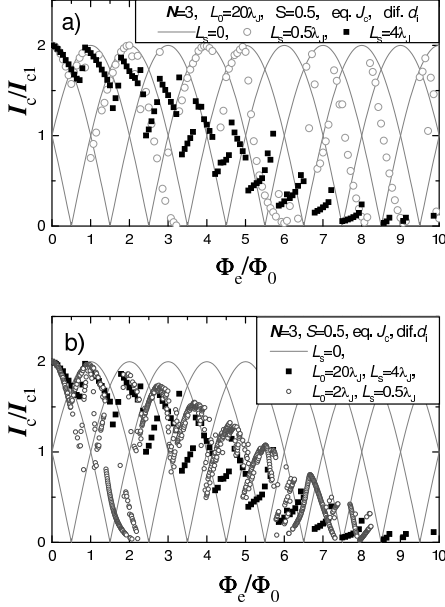


Figure 2. Simulated $I_c(\Phi_e)$ dependence of a SQUID based on $N = 3$ strongly coupled SJJ's for different junction lengths. It is seen that metastability of $I_c(\Phi_e)$ is reduced in moderately long SJJ's SQUID due to magnetic coupling of junctions.

and with boundary conditions that magnetic induction is equal to external field on the outer edges and to the field inside the SQUID loop for the inner edges of SJJ's. Simulations were made for $N = 3$ SJJ's in each SQUID leg. The outer electrodes were assumed to be thicker, $d_{1,4} > d_{2,3}$, in order to model bulk top and bottom bars of the SQUID loop, see Fig. 1.

First we analyze the dependence of current-flux modulation on the in-plane length of the stack, L_S . Fig. 2 shows simulated $I_c(\Phi_e)$ patterns for a SQUID with strongly coupled SJJ's, $S \simeq 0.5$, for different L_S . Parameters of SJJ's are: $d_1 = 0.2\lambda_J$, $d_{2,3} = 0.01\lambda_J$, $d_4 = 0.4\lambda_J$, $t_{1-4} = 0.01\lambda_J$, $\lambda_S = 0.1\lambda_J$, critical current densities of all junctions are identical. In Fig. 2 a) $I_c(\Phi_e)$ patterns are shown for a fixed SQUID loop length, $L_0 = 20\lambda_J$, for short SJJ's $L_S = 0.5\lambda_J$ (open circles) and moderately long SJJ's $L_S = 4\lambda_J$ (solid squares). For comparison, $I_c(\Phi_e)$ for the uncou-

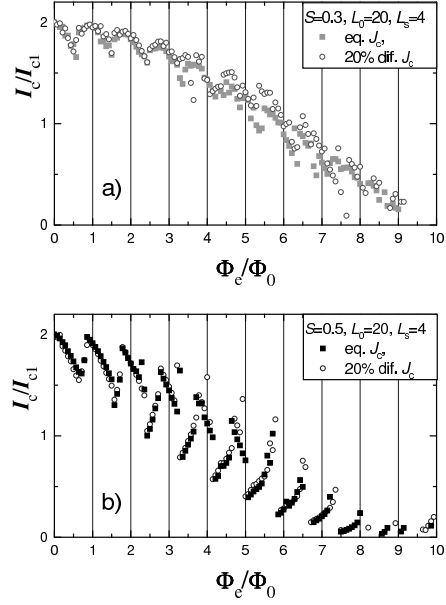


Figure 3. Simulated $I_c(\Phi_e)$ dependence of a SQUID based on $N = 3$ SJJ's for a) moderately coupled and b) strongly coupled SJJ's. It is seen that strongly coupled SJJ's SQUID becomes more stable and less susceptible to the spread in junction parameters.

pled multi-junction SQUID ($L_S = 0$) is shown by thin lines. It is seen that $I_c(\Phi_e)$ of the SQUID with short SJJ's exhibit similar metastability as the uncoupled multi-junction SQUID due to inefficient magnetic coupling in short SJJ's. However, magnetic coupling in moderately long SJJ's strongly reduces metastability of $I_c(\Phi_e)$. An additional large scale modulation of $I_c(\Phi_e)$ in moderately long SJJ's SQUID is due to flux quantization inside SJJ's.

In order to eliminate differences caused by the finite junction length effect, a short SJJ SQUID with a smaller SQUID loop $L_0 = 2\lambda_J$ was also simulated. Results are shown by open circles in Fig. 2 b) along with the data for a moderately long SJJ SQUID from Fig. 2 a). Now finite length effects are similar for both short and long SJJ SQUID's. However, metastability is much more pronounced for a short SJJ SQUID, while

it is strongly suppressed in a moderately long SJJ SQUID.

Next we consider the influence of critical current nonuniformity and the dependence on the coupling strength. In Fig. 3 a) and b) current-flux characteristics of moderately ($S = 0.3$) and strongly ($S = 0.5$) coupled SJJ SQUID's, respectively, are shown for identical J_c 's (solid symbols) and for a 20 % spread in J_c 's (open symbols). In Fig. 3 a) magnetic coupling is reduced due to a larger thickness of middle electrodes, see Eq.(2), $d_{2,3} = 0.1\lambda_J = \lambda_S$, other parameters are the same as in Fig. 2. In the case of nonuniform junctions, $J_{c2} = 1.1J_{c1}$, $J_{c3} = 1.2J_{c1}$.

From Fig. 3 it is seen that $I_c(\Phi_e)$ of a moderately coupled SJJ SQUID is metastable and the performance is further deteriorated by the spread in J_c 's. On the contrary, strongly coupled SJJ SQUID is more stable and less susceptible to a spread in junction parameters.

The increased stability of strongly coupled SJJ SQUIDS can be understood in terms of phase-locking of junctions in the stack. Indeed, the energy difference between states is increased approximately proportional to the number of phase-locked junctions. This was confirmed experimentally by analyzing the "escape rate" in HTSC IJJ's [12]. Another important advantage is that phase-locked junctions switch simultaneously into the resistive state [12]. This creates a possibility for compensation of a reduced current-flux modulation in the multi-junction SQUID by an increased voltage-flux modulation due to phase locking of junctions in the stack.

5. Conclusions

In conclusion, operation of a stacked Josephson junction SQUID is studied numerically. I demonstrate that the coupling between stacked Josephson junctions can improve operation of a multi-junction SQUID:

(i) Metastability of $I_c(\Phi)$ is reduced in SJJs SQUID due to magnetic coupling of junctions.

(ii) Strongly coupled SJJs SQUID becomes more stable and less susceptible to a spread in junction parameters.

(iii) Small $I_c(\Phi)$ modulation can be compen-

sated by an increased voltage-flux response if junctions in the stack are phase-locked.

Finally, some remarks about the optimum SQUID design: Magnetic coupling is effective in long SJJs. However, SJJ's should not be very long, otherwise multiple quasi-equilibrium fluxon modes in SJJ's would strongly complicate flux penetration into the SQUID loop [10,11,8]. The best performance is expected for moderately long SJJ ($L_S \sim 4\lambda_J \sim 2 - 3\mu m$ for Bi-2212). In order to achieve reasonable $I_c(\Phi)$ modulation the number of SJJ's should be kept small (less than ten). This is difficult for HTSC SQUID with the geometry shown in Fig. 1. The solution would be to place the SQUID loop in the ab -plane and form stacks of intrinsic Josephson junctions by cutting trenches, restricting current flow in the ab -plane.

REFERENCES

1. R.Kleiner and P.Müller, Phys. Rev. B 49 (1994) 1327
2. V.M. Krasnov, N.Mros, A.Yurgens and D.Winkler, Phys. Rev. B 59 (1999) 8463
3. V.M. Krasnov, A.Yurgens, D.Winkler, P.Delsing and T.Claeson, Phys. Rev. Lett. 84 (2000) 5860
4. V.M. Krasnov, A.E.Kovalev, A.Yurgens and D.Winkler, Phys. Rev. Lett. 86 (2001) 2657
5. S.J.Lewandowski, Phys.Rev.B 43 (1992) 7776
6. M.Darula, P.Seidel, F.Busse and Š.Beňáčka, J.Appl.Phys. 74 (1993) 2674
7. A.Konopka, S.J.Lewandowski, P.N.Mikheenko and R.Monaco, J.Appl.Phys. 79 (1996) 7871
8. V.M. Krasnov, cond-mat/0109090
9. S.Sakai, P.Bodin and N.F.Pedersen, J. Appl. Phys. **73** (1993) 2411
10. V.M. Krasnov and D. Winkler, Phys. Rev. B **56** (1997) 9106
11. V.M.Krasnov, V.A.Oboznov, V.V.Ryazanov, N.Mros, A.Yurgens and D.Winkler, Phys.Rev.B **61** (2000) 766
12. N.Mros, V.M.Krasnov, A.Yurgens, D.Winkler and T.Claeson, Phys. Rev. B, **57** (1998) R8135